Chapter 2

Kinetic Modeling of the UV/H_2O_2 Process: Determining the Effective Hydroxyl Radical Concentration

Ainhoa Rubio-Clemente, E. Chica and Gustavo A. Peñuela

Additional information is available at the end of the chapter

http://dx.doi.org/10.5772/65096

Abstract

A kinetic model for pollutant degradation by the UV/H_2O_2 system was developed. The model includes the background matrix effect, the reaction intermediate action, and the pH change during time. It was validated for water containing phenol and three different ways of calculating HO° level time-evolution were assumed (non-pseudo-steady, pseudo-steady and simplified pseudo-steady state; denoted as kinetic models A, B and C, respectively). It was found that the kind of assumption considered was not significant for phenol degradation. On the other hand, taking into account the high levels of HO_2° formed in the reaction solution compared to HO° concentration (~10^{-7} M >>>> ~10^{-14} M), HO_2° action in transforming phenol was considered. For this purpose, phenol-HO_2° reaction rate constant was calculated and estimated to be 1.6x10^3 M^{-1} s^{-1}, resulting in the range of data reported from literature. It was observed that, although including HO_2° action allowed slightly improving the kinetic model degree of fit, HO° developed the major role in phenol conversion, due to their high oxidation potential. In this sense, an effective level of HO° can be determined in order to be maintained throughout the UV/H_2O_2 system reaction time for achieving an efficient pollutant degradation.

Keywords: UV/H_2O_2 process, matrix background, kinetic model, reaction rate constant

1. Introduction

Nowadays, one of the major problems associated with the presence of toxic and persistent pollutants in the aquatic environment is the unfeasibility of conventional treatments for the effective removal of those substances [1-3]. Hence the application of alternative technologies,

such as advanced oxidation processes, is needed [4]. Among these techniques, the UV/H_2O_2 system is included. It consists of the photolysis of hydrogen peroxide (H_2O_2) by applying ultraviolet (UV) radiation resulting in the generation of hydroxyl radicals (HO°) [5, 6]. This process may be performed at room temperature and pressure, it has no mass transfer problems, it is easy to maintain and operate, no sludge requiring a subsequent treatment and disposal is produced, and it may achieve a complete pollutant mineralization [5]. Therefore, the UV/H_2O_2 system seems to be a promising alternative for the treatment of water containing toxic and recalcitrant substances. However, this kind of technology can be expensive due to the associated electrical and oxidant costs [7].

In order to reduce costs and make the process more feasible for industrial applications, the UV/H_2O_2 system optimization is required [8] and kinetic models can be considered as functional tools for this purpose. Up to date, several kinetic models have been proposed for describing the UV/H_2O_2 process and predicting different pollutant removal rates [6–15]. In some of these models [13, 15], the proposed set of ordinary differential equations (ODE) defining the studied pollutant degradation rate can be simplified into a pseudo-first–order kinetic expression, whose solution is an exponential one. In such as models, experimental results are fit to that solution. Subsequently, model predictions agree well with laboratory data. In that kind of models the calculated reaction rate constants for the tested pollutant degradation are apparent reaction rate constants (K_{app}), which include pollutant removal reaction rate constants and the values of parameters such as the quantum yield for the oxidant, the conjugate base (HO_2^-), and the contaminant photolysis, the initial level of the chemical species involved in pollutant oxidation, the optical path length of the system, the UV-light intensity, and the molar extinction coefficients of H_2O_2/HO_2^- and pollutant, among others. Therefore, knowing those parameters is not required.

On the other hand, there are dynamic kinetic models that try to solve the considered ODE set, for which the values of the mentioned variables are required, increasing the complexity of the kinetic model. In order to solve the proposed ODE set, the pseudo-steady state approximation assumption for reactive intermediates, such as HO°, is invoked by arguing that these chemical species are as transient ones as their concentration can be presumed to be at a pseudo-steady state [10, 12, 14]. In other models [6–15], on the contrary, the non-pseudo-steady state premise in free radical rate expressions for predicting the degradation of the probe compound in a more accurate way is applied. However, although hydroperoxyl radicals (HO_2°) are involved in those models, none of them, excluding Huang and Shu [11] and Liao and Gurol [12] models, includes HO_2° in the target pollutant oxidation final expression. Additionally, some of these models cannot be reproduced unless a conversion factor is included, as demonstrated by Audenaert et al. [8].

In this sense, the aim of this work was to develop a kinetic model based on the main chemical and photochemical reactions for pollutant degradation in water systems by the UV/H_2O_2 process taking into account the decomposition of the pollutant through direct photolysis, HO° oxidation, and HO_2° and superoxide radical ($O_2^{\cdot-}$) transformation. Furthermore, HO° scavenging effects of carbonate (CO_3^{2-}), bicarbonate (HCO_3^-), sulfate (SO_4^{2-}), and chloride (Cl^-) ions were considered. pH changes in the bulk and the detrimen-

http://dx.doi.org/10.5772/65096

tal action of the organic matter (OM) and the reaction intermediates in shielding UV and quenching HO° were studied. The influence of the pseudo-steady and non-pseudo-steady state hypothesis for determining HO° concentration-evolution with time was also examined and the second-order HO_2° reaction rate constant for the studied pollutant was determined. MATLAB software was used to solve the ODE set that characterizes the current model and the results were validated by using experimental data obtained from the literature for phenol (PHE) degradation by the UV/H_2O_2 process in a completely mixed batch photoreactor.

2. Experimental model approach

A mathematical model for predicting pollutant degradation and the concentrations of the main species involved in a UV/H_2O_2 system was developed. The developed model describes radical chain reactions occurring during the UV/H_2O_2 process in the presence of HO° scavengers and UV-radiation absorbers, such as dissolved organic matter (DOM), anions and reaction intermediate products. Pollutant degradation mechanisms, direct UV photolysis and radical attack by HO°, HO_2°, $O_2^{\circ-}$ and other anion radicals ($CO_3^{\circ-}$, $SO_4^{\circ-}$, H_2ClO°, HClO°, Cl°, and $Cl_2^{\circ-}$) were included. Additionally, the model incorporates the competitive UV-radiation absorption by H_2O_2, the parent compound and the DOM in terms of dissolved organic carbon (DOC), as well as the formation and disappearance of intermediate products, also considered as DOC. Moreover, it accounts for the solution pH change due to the mineralization of organic compounds and the formation of acids.

2.1. UV/H_2O_2 system fundamentals

The UV/H_2O_2 system initiates with the primary photolysis of H_2O_2 or HO_2^-, producing HO° according to Eqs. (1) and (2) [6, 13]. Based on the Beer-Lambert law and quantum yield definition, the reaction rates for H_2O_2/HO_2^- direct photodegradation and HO° generation are obtained through Eqs. (3)—(5), respectively.

$$H_2O_2 \xrightarrow{h\upsilon} 2HO^\circ \tag{1}$$

$$HO_2^- + H_2O \xrightarrow{h\upsilon} 2HO^\circ + OH^- \tag{2}$$

$$\frac{d[H_2O_2]}{dt} = -\phi_{H_2O_2} I_{a,\,H_2O_2} \tag{3}$$

$$\frac{d\left[\mathrm{HO}_2^-\right]}{dt} = -\phi_{\mathrm{HO}_2^-} I_{a,\,\mathrm{HO}_2^-} \tag{4}$$

$$\frac{d\left[\mathrm{HO}^\circ\right]}{dt} = 2\phi_{\mathrm{H_2O_2}} I_{a,\,\mathrm{H_2O_2}} + 2\phi_{\mathrm{HO}_2^-} I_{a,\,\mathrm{HO}_2^-} \tag{5}$$

where $\phi_{H_2O_2}$ and $\phi_{HO^-_2}$ (mol Ein^{-1}) are the quantum yields of the photochemical reactions of H_2O_2 and HO_2^-. $I_{a,\,H_2O_2}$ and $I_{a,\,HO^-_2}$ (Ein L^{-1} s^{-1}) refer to the UV-radiation intensities absorbed by H_2O_2 and HO_2^-, respectively, calculated according to Eqs. (6) and (7), where $f_{H_2O_2}$ and $f_{HO^-_2}$ are the fractions of the UV-radiation absorbed by H_2O_2 and HO_2^-, respectively (Eqs. (8) and (9)) [7, 8].

$$I_{a,H_2O_2} = I_0 f_{H_2O_2}\{1 - exp[-2.3l(\varepsilon_{H_2O_2}[H_2O_2] + \varepsilon_{HO_2^-}[HO_2^-] + \varepsilon_C[C] + \varepsilon_{DOC}[DOC])]\} \tag{6}$$

$$I_{a,\mathrm{HO}_2^-} = I_0 f_{\mathrm{HO}_2^-}\left\{1 - exp\left[-2.3l\left(\varepsilon_{\mathrm{H_2O_2}}\left[\mathrm{H_2O_2}\right] + \varepsilon_{\mathrm{HO}_2^-}\left[\mathrm{HO}_2^-\right] + \varepsilon_C\left[\mathrm{C}\right] + \varepsilon_{\mathrm{DOC}}\left[\mathrm{DOC}\right]\right)\right]\right\} \tag{7}$$

$$f_{\mathrm{H_2O_2}} = \frac{\varepsilon_{\mathrm{H_2O_2}}\left[\mathrm{H_2O_2}\right]}{\varepsilon_{\mathrm{H_2O_2}}\left[\mathrm{H_2O_2}\right] + \varepsilon_{\mathrm{HO}_2^-}\left[\mathrm{HO}_2^-\right] + \varepsilon_{\mathrm{C}}\left[\mathrm{C}\right] + \varepsilon_{\mathrm{DOC}}\left[\mathrm{DOC}\right]} \tag{8}$$

$$f_{\mathrm{HO}_2^-} = \frac{\varepsilon_{\mathrm{HO}_2^-}\left[\mathrm{HO}_2^-\right]}{\varepsilon_{\mathrm{H_2O_2}}\left[\mathrm{H_2O_2}\right] + \varepsilon_{\mathrm{HO}_2^-}\left[\mathrm{HO}_2^-\right] + \varepsilon_{\mathrm{C}}\left[\mathrm{C}\right] + \varepsilon_{\mathrm{DOC}}\left[\mathrm{DOC}\right]} \tag{9}$$

in which $[H_2O_2]$, $[HO_2^-]$, [C], and [DOC] are H_2O_2, HO_2^-, contaminant and DOM, in terms of DOC, concentrations, respectively. $\varepsilon_{H_2O_2}$, $\varepsilon_{HO_2^-}$, ε_C and ε_{DOC} (M^{-1} m^{-1}) are the molar extinction coefficients of H_2O_2, HO_2^-, the pollutant and the DOC, respectively. In turn, l (mm) is the photoreactor path length and I_0 (Ein s^{-1}), the incident UV-light intensity.

In addition to the oxidant photolysis, the target pollutant (C) may interact with the UV-radiation, undergoing degradation and producing reaction intermediates. A fraction of those by-products can be dissolved in the solution [16]. This fraction is denoted as DOC (Eq. (10)) [6]. The reaction rate for the contaminant direct photolysis is obtained through Eq. (11).

$$\mathrm{C} \xrightarrow{h\upsilon} \mathrm{DOC} + ? \tag{10}$$

http://dx.doi.org/10.5772/65096

$$\frac{d[\mathrm{C}]}{dt} = -\phi_c I_{a,\,\mathrm{C}} \tag{11}$$

where ϕ_{C} is the quantum yield of pollutant photolysis and $I_{a,\,\mathrm{C}}$ is the amount of UV-light absorbed by the contaminant, calculated through Eqs. (12) and (13).

$$I_{a,\,\mathrm{C}} = I_0 f_{\mathrm{C}} \left\{1 - \exp\left[-2.3l\left(\varepsilon_{\mathrm{H_2O_2}}[\mathrm{H_2O_2}] + \varepsilon_{\mathrm{HO_2^-}}\left[\mathrm{HO_2^-}\right] + \varepsilon_{\mathrm{C}}[\mathrm{C}] + \varepsilon_{\mathrm{DOC}}[\mathrm{DOC}]\right)\right]\right\} \tag{12}$$

$$f_{\mathrm{C}} = \frac{\varepsilon_{\mathrm{C}}[\mathrm{C}]}{\varepsilon_{\mathrm{H_2O_2}}[\mathrm{H_2O_2}] + \varepsilon_{\mathrm{HO_2^-}}\left[\mathrm{HO_2^-}\right] + \varepsilon_{\mathrm{C}}[\mathrm{C}] + \varepsilon_{\mathrm{DOC}}[\mathrm{DOC}]} \tag{13}$$

Once HO° are produced, they rapidly react with the pollutant of interest, degrading it to form reaction intermediates (Eq. (14)), which subsequently can be attacked by HO° and undergo further degradation to produce final products, such as CO_2, H_2O, and mineral acids (Eq. (15)) [7]. In this model, intermediate substances were considered as HO° scavengers as well as UV-light absorbers. Additionally, it was assumed that the pH of the solution decreased due to the conversion of the target pollutant, and consequently the reaction intermediates, into carbon dioxide (i.e., $H_2CO_3^*$ in the aqueous phase); although it must be highlighted that not all the DOC is mineralized, since carboxylic acids are also formed during the oxidation process, making the pH of the bulk decreases as well [8]. Under this presumption, Eq. (15) is simplified as Eq. (16). The mass balances for the evolution of the pollutant, the dissolved organic fraction of the formed by-products, HO° and the $H_2CO_3^*$ concentrations with time are shown by Eqs. (17)–(20), respectively.

$$\mathrm{C} + \mathrm{HO}^\circ \xrightarrow{k_{\mathrm{C,HO}^\circ}} \mathrm{DOC} + ? \tag{14}$$

$$\mathrm{DOC} + \mathrm{HO}^\circ \xrightarrow{k_{\mathrm{DOC,\,HO}^\circ}} \mathrm{CO_2} + \mathrm{H_2O} + \text{mineral acids} \tag{15}$$

$$\mathrm{DOC} + \mathrm{HO}^\circ \xrightarrow{k_{\mathrm{DOC,\,HO}^\circ}} \mathrm{H_2CO_3^*} + \mathrm{H_2O} \tag{16}$$

$$\frac{d[\mathrm{C}]}{dt} = -k_{\mathrm{C,HO^\circ}}[\mathrm{HO^\circ}][\mathrm{C}] \tag{17}$$

$$\frac{d[\mathrm{DOC}]}{dt} = k_{\mathrm{C,HO^\circ}}[\mathrm{HO^\circ}][\mathrm{C}] - k_{\mathrm{DOC,HO^\circ}}[\mathrm{HO^\circ}][\mathrm{DOC}] \tag{18}$$

$$\frac{d[HO^\circ]}{dt} = -k_{\mathrm{C,\ HO^\circ}}[\mathrm{HO^\circ}][\mathrm{C}] - k_{\mathrm{DOC,\ HO^\circ}}[\mathrm{HO^\circ}][\mathrm{DOC}] \tag{19}$$

$$\frac{d\left[\mathrm{H_2CO_3^*}\right]}{dt} = k_{\mathrm{DOC,HO^\circ}}[\mathrm{HO^\circ}][\mathrm{DOC}] \tag{20}$$

where [C], [DOC], [HO°], and [$H_2CO_3^*$] correspond to pollutant, dissolved by-products, HO° and $H_2CO_3^*$ levels, respectively. k_{C,HO° and k_{DOC,HO° are the rate constants of Eq. (14) and (15) or (16).

In the UV/H_2O_2 system, recombination of HO° can occur to produce H_2O_2. However, these free radicals can also react with H_2O_2 and HO_2^-, particularly when the oxidant is in excess, to produce HO_2°. Although HO_2° are less reactive than HO° (E° = 0.98 and 2.8 V, respectively) [8], they can also be involved in pollutant degradation, especially if these radicals are produced in high amounts in the system. Furthermore, HO_2° can produce $O_2^{\circ-}$, which subsequently can participate in pollutant degradation and mineralization [17]. Therefore, the role of these reactive oxygen species was included in the proposed kinetic model.

It is important to note that as the oxidation process develops, the pH of the solution generally goes down, and consequently, some chemical species appear while other species vanish. In order to consider the change of chemical species inside the bulk according to the pH of the solution in the kinetic model, a correction factor (δ_{R_i}) was introduced for the photolysis of H_2O_2, HO_2^-, and for the reaction between H_2O_2 and HO°. This correction factor can adopt two values (0 and 1). When δ_{R_i}=1, reaction R_i is promoted (i.e., the time-varying concentrations of the chemical species involved in reaction R_i are taken into account in the model). When δ_{R_i}=0, reaction R_i is not considered in the model and, subsequently, the chemical species taking part in reaction R_i are neglected.

On the other hand, species commonly present in water, such as DOM and inorganic anions (e.g., CO_3^{2-}, HCO_3^-, SO_4^{2-}, and Cl^-, among others) may also have a significant effect because of their ability to absorb UV-light and/or to scavenge HO°. The HO° scavenging effect of matrix

http://dx.doi.org/10.5772/65096

constituents drastically limits the oxidation action of HO°, leading to a decrease in the performance of the system [18].

Taking into account all the mentioned processes and in order to give a more realistic view of what happens in the UV/H_2O_2 process, the kinetic equation describing pollutant degradation can be expressed as Eq. (21).

$$-\frac{d\mathrm{C}}{dt} = \phi_c I_{a,\,\mathrm{C}} + k_{14}[\mathrm{C}][\mathrm{HO}^\circ] + k_{15}[\mathrm{C}]\left[\mathrm{HO}_2^\circ\right] + k_{16}[\mathrm{C}]\left[\mathrm{O}_2^{\circ-}\right] + \sum_{i=35}^{40} k_i[\mathrm{C}][\mathrm{AR}_i] \qquad (21)$$

where the terms $\phi_c I_{a,\,\mathrm{C}}$, $k_{14}[\mathrm{C}][\mathrm{HO}^\circ]$, $k_{15}[\mathrm{C}]\left[\mathrm{HO}_2^\circ\right]$, $k_{16}[\mathrm{C}]\left[\mathrm{O}_2^{\circ-}\right]$ and $\sum_{i=35}^{40} k_i[\mathrm{C}]\left[\mathrm{AR}_i\right]$ represent the specific contributions of UV-radiation, the oxidation of HO°, HO_2°, O_2°$^-$ and the formed anion radicals (AR) (including CO_3°$^-$, SO_4°$^-$, H_2ClO°, HClO°, Cl°, and Cl_2°$^-$) to the overall pollutant degradation, respectively.

In order to quantitatively evaluate the contribution of the cited terms in the contaminant removal, parameters *d*, *f*, *g*, and *h* were introduced in Eq. (21), as described by Eq. (22).

$$-\frac{dC}{dt} = \phi_c I_{a,\,\mathrm{C}} + k_{14}[\mathrm{C}][\mathrm{HO}^\circ]d + k_{15}[\mathrm{C}]\left[\mathrm{HO}_2^\circ\right]f + k_{16}[\mathrm{C}]\left[\mathrm{O}_2^{\circ-}\right]g + \sum_{i=35}^{40} k_i[\mathrm{C}][\mathrm{AR}_i]h \qquad (22)$$

When $d = f = g = h = 0$ (i.e., when the initial concentrations of oxidant radical species are equal to zero), the kinetic model only describes the degradation of the pollutant by photolysis. If $d = h = 1$ and $f = g = 0$, in addition to the photolysis conversion, in a deionized water, the model can predict pollutant transformation through HO° and CO_3°$^-$ (the latter from the reaction between HO° and HCO_3^- or CO_3^{2-}). When $d = f = h = 1$ and g = 0, contaminant removal by photolysis and the action of HO° and HO_2°, as well as CO_3°$^-$, is described. When all the parameters are equal to 1 (i.e., $d = f = g = h = 1$) and there are no inorganic anions different from HCO_3^- and CO_3^{2-} in the studied water, the kinetic model accounts for the degradation of the pollutant by direct photolysis and oxidation through HO°, HO_2°, O_2°$^-$, and CO_3°$^-$. As the model includes the reactions where Cl^-, SO_4^{2-}, CO_3^{2-}, and HCO_3^- are involved, it can be used for the treatment of different types of water.

Based on the reactions illustrated in **Figures 1** and **2**, and the different involved parameters, the mass balances and the corresponding ODE of the species of interest (C, DOC, H_2O_2, HO_2^-, HO°, HO_2°, O_2°$^-$, CO_3°$^-$, SO_4°$^-$, HClO°$^-$, H_2ClO°, HClO°, Cl°, Cl_2°$^-$, OH^-, H^+, $H_2CO_3^*$, CO_3^{2-}, HCO_3^-, HSO_4^-, SO_4^{2-}, and Cl^-) are summarized in **Table 1**.

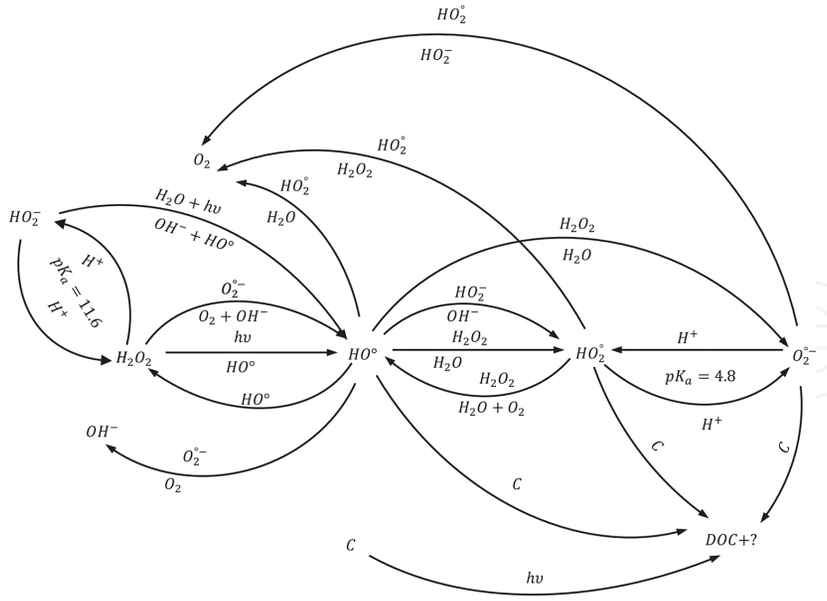

Figure 1. Reaction network of the UV/H_2O_2 process for the degradation of the parent compound without considering the effect of matrix constituents. The species above and below the arrows are the co-reactants and the co-products, respectively.

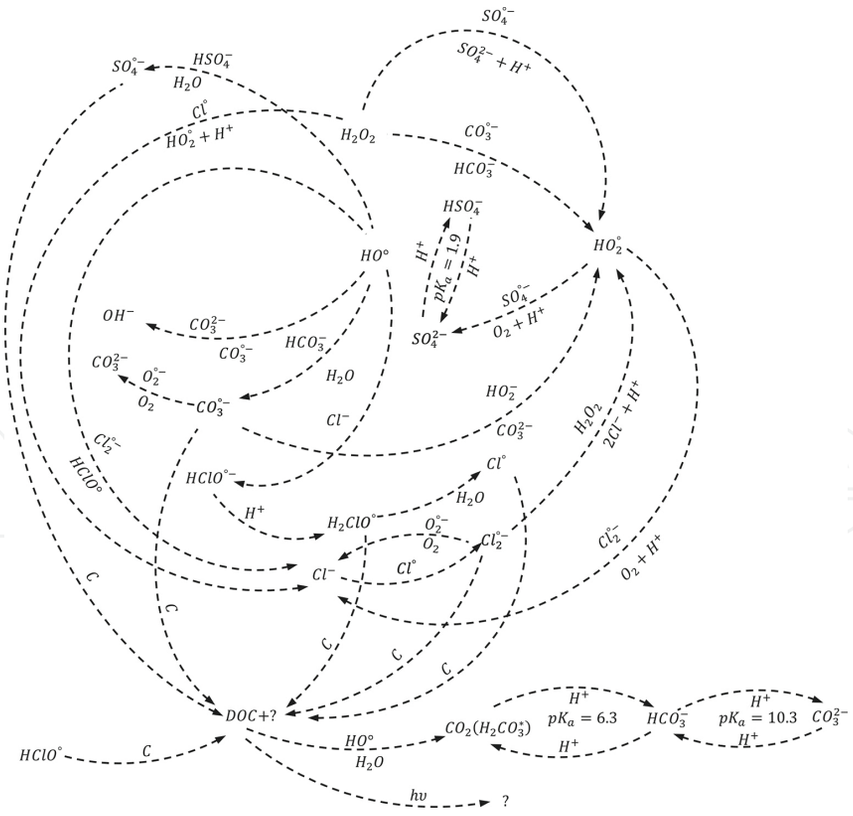

Figure 2. Reaction network describing the effect of the matrix background in the UV/H_2O_2 system with co-reactants and co-products above and below the arrows, respectively.

http://dx.doi.org/10.5772/65096

No.	Species	Kinetic expressions
ODE_1	C	$\frac{d[C]}{dt} = -\phi_c I_{a,C} - k_{14}[C][HO^\circ]d - k_{15}[C][HO_2^\circ]f - k_{16}[C][O_2^{\circ-}]g - (k_{35}[C][CO_3^{\circ-}]+k_{36}[C][SO_4^{\circ-}]+k_{37}[C][H_2ClO^\circ]+k_{38}[C][HClO^\circ]+k_{39}[C][Cl^\circ]+k_{40}[C][Cl_2^{\circ-}])h$
ODE_2	H_2O_2	$\frac{d[H_2O_2]}{dt} = -\phi_{H_2O_2} I_{a,H_2O_2}\delta_{R_3} - k_1[H_2O_2] + k_2[HO_2^-][H^+] - k_5[H_2O_2][HO^\circ]\delta_{R_7} - k_5[H_2O_2][HO^\circ]\delta_{R_8} + k_7[^\circ OH][HO^\circ] + k_{10}[HO_2^\circ][HO_2^\circ] - k_{11}[H_2O_2][HO_2^\circ] - k_{12}[H_2O_2][O_2^{\circ-}] - k_{20}[H_2O_2][CO_3^{\circ-}] - k_{24}[SO_4^{\circ-}][H_2O_2] - k_{31}[Cl_2^{\circ-}][H_2O_2] - k_{32}[Cl^\circ][H_2O_2]$
ODE_3	HO_2^-	$\frac{d[HO_2^-]}{dt} = -\phi_{HO_2^-} I_{a,HO_2^-}\delta_{R_4} + k_1[H_2O_2] - k_2[HO_2^-][H^+] - k_6[HO^\circ][HO_2^-] + k_{13}[HO_2^\circ][O_2^{\circ-}] - k_{21}[HO_2^-][CO_3^{\circ-}]$
ODE_4	$^\circ OH$	$\frac{d[HO^\circ]}{dt} = 2\phi_{H_2O_2} I_{a,H_2O_2}\delta_{R_3} + 2\phi_{HO_2^-} I_{a,HO_2^-}\delta_{R_4} - k_5[H_2O_2][HO^\circ]\delta_{R_7} - k_5[H_2O_2][HO^\circ]\delta_{R_8} - k_6[HO^\circ][HO_2^-] - k_7[HO^\circ][HO^\circ] - k_8[HO^\circ][HO_2^\circ] - k_9[HO^\circ][O_2^{\circ-}] + k_{11}[H_2O_2][HO_2^\circ] + k_{12}[H_2O_2][O_2^{\circ-}] - k_{14}[C][HO^\circ]d - k_{17}[DOC][HO^\circ] - k_{18}[CO_3^{2-}][HO^\circ] - k_{19}[HCO_3^-][HO^\circ] - k_{23}[HSO_4^-][HO^\circ] - k_{26}[Cl^-][HO^\circ] - k_{30}[Cl_2^{\circ-}][HO^\circ]$
ODE_5	HO_2°	$\frac{d[HO_2^\circ]}{dt} = -k_3[HO_2^\circ] + k_4[O_2^{\circ-}][H^+] + k_5[H_2O_2][HO^\circ]\delta_{R_8} + k_6[HO^\circ][HO_2^-] - k_8[HO^\circ][HO_2^\circ] - k_{10}[HO_2^\circ][HO_2^\circ] - k_{11}[H_2O_2][HO_2^\circ] - k_{13}[HO_2^\circ][O_2^{\circ-}] - k_{15}[C][HO_2^\circ]f + k_{20}[H_2O_2][CO_3^{\circ-}] + k_{21}[HO_2^-][CO_3^{\circ-}] + k_{24}[SO_4^{\circ-}][H_2O_2] - k_{25}[SO_4^{\circ-}][HO_2^\circ] + k_{31}[Cl_2^{\circ-}][H_2O_2] + k_{32}[Cl^\circ][H_2O_2] - k_{33}[Cl_2^{\circ-}][HO_2^\circ]$
ODE_6	$O_2^{\circ-}$	$\frac{d[O_2^{\circ-}]}{dt} = k_3[HO_2^\circ] - k_4[O_2^{\circ-}][H^+] + k_5[H_2O_2][HO^\circ]\delta_{R_7} - k_9[HO^\circ][O_2^{\circ-}] - k_{12}[H_2O_2][O_2^{\circ-}] - k_{13}[HO_2^\circ][O_2^{\circ-}] - k_{16}[C][O_2^{\circ-}]g - k_{22}[O_2^{\circ-}][CO_3^{\circ-}] - k_{34}[Cl_2^{\circ-}][O_2^{\circ-}]$
ODE_7	OH^-	$\frac{d[OH^-]}{dt} = \phi_{HO_2^-} I_{a,HO_2^-}\delta_{R_4} + k_6[HO^\circ][HO_2^-] + k_9[HO^\circ][O_2^{\circ-}] + k_{12}[H_2O_2][O_2^{\circ-}] + k_{18}[CO_3^{2-}][HO^\circ]$
ODE_8	H^+	$\frac{d[H^+]}{dt} = k_1[H_2O_2] - k_2[HO_2^-][H^+] + k_3[HO_2^\circ] - k_4[O_2^{\circ-}][H^+] + k_5[H_2O_2][HO^\circ]\delta_{R_7} + k_{24}[SO_4^{\circ-}][H_2O_2] + k_{25}[SO_4^{\circ-}][HO_2^\circ] - k_{27}[HClO^{\circ-}][H^+] + k_{31}[Cl_2^{\circ-}][H_2O_2] + k_{32}[Cl^\circ][H_2O_2] + k_{33}[Cl_2^{\circ-}][HO_2^\circ] + k_{41}[H_2CO_3^\circ] - k_{42}[HCO_3^-][H^+] + k_{43}[HCO_3^-] - k_{44}[CO_3^{2-}][H^+] + k_{45}[HSO_4^-] - k_{46}[SO_4^{2-}][H^+]$
ODE_9	DOC	$\frac{d[DOC]}{dt} = \phi_c I_{a,C} + k_{14}[C][HO^\circ]d + k_{15}[C][HO_2^\circ]f + k_{16}[C][O_2^{\circ-}]g - k_{17}[DOC][HO^\circ] - \phi_{DOC} I_{a,DOC} + (k_{35}[C][CO_3^{\circ-}] + k_{36}[C][SO_4^{\circ-}] + k_{37}[C][H_2ClO^\circ]+k_{38}[C][HClO^\circ] + k_{39}[C][Cl^\circ] + k_{40}[C][Cl_2^{\circ-}])h$
ODE_{10}	CO_3^{2-}	$\frac{d[CO_3^{2-}]}{dt} = -k_{18}[CO_3^{2-}][HO^\circ] + k_{21}[HO_2^-][CO_3^{\circ-}] + k_{22}[O_2^{\circ-}][CO_3^{\circ-}] + k_{43}[HCO_3^-] - k_{44}[CO_3^{2-}][H^+]$
ODE_{11}	$CO_3^{\circ-}$	$\frac{d[CO_3^{\circ-}]}{dt} = k_{18}[CO_3^{2-}][HO^\circ] + k_{19}[HCO_3^-][HO^\circ] - k_{20}[H_2O_2][CO_3^{\circ-}] - k_{21}[HO_2^-][CO_3^{\circ-}] - k_{22}[O_2^{\circ-}][CO_3^{\circ-}] - k_{35}[C][CO_3^{\circ-}]h$

ODE_{12}	HCO_3^-	$\frac{d[HCO_3^-]}{dt} = -k_{19}[HCO_3^-][HO^\circ] + k_{20}[H_2O_2][CO_3^{\circ-}] + k_{41}[H_2CO_3^*] - k_{42}[HCO_3^-][H^+] - k_{43}[HCO_3^-] + k_{44}[CO_3^{2-}][H^+]$
ODE_{13}	$H_2CO_3^*$	$\frac{d[H_2CO_3^*]}{dt} = k_{17}[DOC][HO^\circ] - k_{41}[H_2CO_3^*] + k_{42}[HCO_3^-][H^+]$
ODE_{14}	HSO_4^-	$\frac{d[HSO_4^-]}{dt} = -k_{23}[HSO_4^-][HO^\circ] - k_{45}[HSO_4^-] + k_{46}[SO_4^{2-}][H^+]$
ODE_{15}	$SO_4^{\circ-}$	$\frac{d[SO_4^{\circ-}]}{dt} = k_{23}[HSO_4^-][HO^\circ] - k_{24}[SO_4^{\circ-}][H_2O_2] - k_{25}[SO_4^{\circ-}][HO_2^\circ] - k_{36}[C][SO_4^{\circ-}]h$
ODE_{16}	SO_4^{2-}	$\frac{d[SO_4^{2-}]}{dt} = k_{24}[SO_4^{\circ-}][H_2O_2] + k_{25}[SO_4^{\circ-}][HO_2^\circ] + k_{45}[HSO_4^-] - k_{46}[SO_4^{2-}][H^+]$
ODE_{17}	Cl^-	$\frac{d[Cl^-]}{dt} = -k_{26}[Cl^-][HO^\circ] - k_{29}[Cl^\circ][Cl^-] + k_{30}[Cl_2^{\circ-}][^\circ OH] + 2k_{31}[Cl_2^{\circ-}][H_2O_2] + k_{32}[Cl^\circ][H_2O_2] + 2k_{33}[Cl_2^{\circ-}][HO_2^\circ] + 2k_{34}[Cl_2^{\circ-}][O_2^{\circ-}]$
ODE_{18}	$HClO^{\circ-}$	$\frac{d[HClO^{\circ-}]}{dt} = k_{26}[Cl^-][HO^\circ] - k_{27}[HClO^{\circ-}][H^+]$
ODE_{19}	H_2ClO°	$\frac{d[H_2ClO^\circ]}{dt} = k_{27}[HClO^{\circ-}][H^+] - k_{28}[H_2ClO^\circ] - k_{37}[C][H_2ClO^\circ]h$
ODE_{20}	$HClO^\circ$	$\frac{d[HClO^\circ]}{dt} = k_{30}[Cl_2^{\circ-}][HO^\circ] - k_{38}[C][HClO^\circ]h$
ODE_{21}	Cl°	$\frac{d[Cl^\circ]}{dt} = k_{28}[H_2ClO^\circ] - k_{29}[Cl^\circ][Cl^-] - k_{32}[Cl^\circ][H_2O_2] - k_{39}[C][Cl^\circ]h$
ODE_{22}	$Cl_2^{\circ-}$	$\frac{d[Cl_2^{\circ-}]}{dt} = k_{29}[Cl^\circ][Cl^-] - k_{30}[Cl_2^{\circ-}][HO^\circ] - k_{31}[Cl_2^{\circ-}][H_2O_2] - k_{33}[Cl_2^{\circ-}][HO_2^\circ] - k_{34}[Cl_2^{\circ-}][O_2^{\circ-}] - k_{40}[C][Cl_2^{\circ-}]h$
k_i		$k_1 = 3.7\text{x}10^{-2}\ s^{-1}$; $k_2 = 2.6\text{x}10^{10}\ M^{-1}s^{-1}$; $\varepsilon_{H_2O_2}(254\ nm) = 1\ 800\ M^{-1}m^{-1}$; $\varepsilon_{HO_2^-}(254\ nm) = 22\ 800\ M^{-1}m^{-1}$; $\phi_{H_2O_2}(254\ nm) = 0.5\ molEin^{-1}$; $\phi_{HO_2^-}(254\ nm) = 0.5\ molEin^{-1}$; $pH > 11.6 \Rightarrow \delta_{R_3} = 0, \delta_{R_4} = 1$; $pH < 11.6 \Rightarrow \delta_{R_3} = 1, \delta_{R_4} = 0$; $k_3 = 1.58\text{x}10^5\ s^{-1}$; $k_4 = 1.0\text{x}10^{10}\ M^{-1}s^{-1}$; $k_5 = 2.7\text{x}10^7\ M^{-1}s^{-1}$; $pH > 4.8 \Rightarrow \delta_{R_7} = 1, \delta_{R_8} = 0$; $pH < 4.8 \Rightarrow \delta_{R_7} = 0, \delta_{R_8} = 1$; $k_6 = 7.5\text{x}10^9\ M^{-1}s^{-1}$; $k_7 = 5.5\text{x}10^9\ M^{-1}s^{-1}$; $k_8 = 6.6\text{x}10^9\ M^{-1}s^{-1}$; $k_9 = 7.0\text{x}10^9\ M^{-1}s^{-1}$; $k_{10} = 8.3\text{x}10^5\ M^{-1}s^{-1}$; $k_{11} = 3\ M^{-1}s^{-1}$; $k_{12} = 0.13\ M^{-1}s^{-1}$; $k_{13} = 9.7\text{x}10^7\ M^{-1}s^{-1}$; $k_{C,\ HO^\circ} = k_{14}$; $k_{C,HO_2^\circ} = k_{15}$; $k_{C,O_2^{\circ-}} = k_{16}$; $k_{DOC,\ HO^\circ} = k_{17} = 2.0\text{x}10^8\ M^{-1}s^{-1}$; $k_{18} = 3.9\text{x}10^8\ M^{-1}s^{-1}$; $k_{19} = 8.5\text{x}10^6\ M^{-1}s^{-1}$; $k_{20} = 4.3\text{x}10^5\ M^{-1}s^{-1}$; $k_{21} = 3.0\text{x}10^7\ M^{-1}s^{-1}$; $k_{22} = 6.5\text{x}10^8\ M^{-1}s^{-1}$; $k_{23} = 3.5\text{x}10^5\ M^{-1}s^{-1}$; $k_{24} = 1.2\text{x}10^7\ M^{-1}s^{-1}$; $k_{25} = 3.5\text{x}10^9\ M^{-1}s^{-1}$; $k_{26} = 4.3\text{x}10^9\ M^{-1}s^{-1}$; $k_{27} = 3.0\text{x}10^{10}\ M^{-1}s^{-1}$; $k_{28} = 5.0\text{x}10^4\ s^{-1}$; $k_{29} = 8.5\text{x}10^9\ M^{-1}s^{-1}$; $k_{30} = 1.0\text{x}10^9\ M^{-1}s^{-1}$; $k_{31} = 4.1\text{x}10^4\ M^{-1}s^{-1}$; $k_{32} = 1.1\text{x}10^9\ M^{-1}s^{-1}$; $k_{33} = 3.0\text{x}10^9\ M^{-1}s^{-1}$; $k_{34} = 2.0\text{x}10^9\ M^{-1}s^{-1}$; $k_{35} = ?$; $k_{36} = ?$; $k_{37} = ?$; $k_{38} = ?$; $k_{39} = ?$; $k_{40} = ?$; $k_{41} = 1\text{x}10^{10}\ s^{-1}$; $k_{42} = 4.5\text{x}10^3\ M^{-1}s^{-1}$; $k_{43} = 1\text{x}10^{10}\ s^{-1}$; $k_{44} = 4.5\text{x}10^{-1}\ M^{-1}s^{-1}$; $k_{45} = 1\text{x}10^{10}\ s^{-1}$; $k_{46} = 4.5\text{x}10^{11}\ M^{-1}s^{-1}$

Table 1. Set of the ODE used in the kinetic model [9, 18, 27, 30–39].

http://dx.doi.org/10.5772/65096

2.2. Proposed kinetic model

In the developed kinetic model, three different ways of calculating the evolution of HO° concentration during time were presumed: (a) a non-pseudo-steady or transient state (i.e., the net formation rate of HO° is different from zero); (b) a pseudo-steady state; and (c) a simplified pseudo-steady state; correspondingly denoted as kinetic model A, B, and C.

In the prediction model A the concentration of HO° can be calculated with Eq. (23). From Eq. (23), the HO° concentration can be written as Eq. (24) (prediction model B).

$$\begin{aligned}\frac{d[\mathrm{HO}^\circ]}{dt} &= 2\phi_{\mathrm{H_2O_2}} I_{a,\,\mathrm{H_2O_2}} \delta_{R_3} + 2\phi_{\mathrm{HO_2^-}} I_{a,\mathrm{HO_2^-}} \delta_{R_4} - k_5[\mathrm{H_2O_2}][\mathrm{HO}^\circ]\delta_{R_7} - \\ & k_5[\mathrm{H_2O_2}][\mathrm{HO}^\circ]\delta_{R_8} - k_6[\mathrm{HO}^\circ]\left[\mathrm{HO_2^-}\right] - k_7[\mathrm{HO}^\circ][\mathrm{HO}^\circ] - k_8[\mathrm{HO}^\circ]\left[\mathrm{HO_2^\circ}\right] - \\ & k_9[\mathrm{HO}^\circ]\left[\mathrm{O_2^{\circ -}}\right] + k_{11}[\mathrm{H_2O_2}]\left[\mathrm{HO_2^\circ}\right] + k_{12}[\mathrm{H_2O_2}]\left[\mathrm{O_2^{\circ -}}\right] - k_{14}[\mathrm{C}][\mathrm{HO}^\circ]d - \\ & k_{17}[\mathrm{DOC}][\mathrm{HO}^\circ] - k_{18}\left[\mathrm{CO_3^{2-}}\right][\mathrm{HO}^\circ] - k_{19}\left[\mathrm{HCO_3^-}\right][\mathrm{HO}^\circ] - k_{23}\left[\mathrm{HSO_4^-}\right][\mathrm{HO}^\circ] - \\ & k_{26}\left[\mathrm{Cl^-}\right][\mathrm{HO}^\circ] - k_{30}\left[\mathrm{Cl_2^{\circ -}}\right][\mathrm{HO}^\circ]\end{aligned} \tag{23}$$

$$\begin{aligned}[\mathrm{HO}^\circ] = {} & (2\phi_{\mathrm{H_2O_2}} I_{a,\,\mathrm{H_2O_2}} \delta_{R_3} + 2\phi_{\mathrm{HO_2^-}} I_{a,\,\mathrm{HO_2^-}} \delta_{R_4} + k_{11}[\mathrm{H_2O_2}]\left[\mathrm{HO_2^\circ}\right] + k_{12}[\mathrm{H_2O_2}]\left[\mathrm{O_2^{\circ -}}\right]) / \\ & (k_5[\mathrm{H_2O_2}]\delta_{R_7} + k_5[\mathrm{H_2O_2}]\delta_{R_8} + k_6\left[\mathrm{HO_2^-}\right] + k_8\left[\mathrm{HO_2^\circ}\right] + k_9\left[\mathrm{O_2^{\circ -}}\right] + k_{14}[\mathrm{C}]d + \\ & k_{17}[\mathrm{DOC}] + k_{18}\left[\mathrm{CO_3^{2-}}\right] + k_{19}\left[\mathrm{HCO_3^-}\right] + k_{23}\left[\mathrm{HSO_4^-}\right] + k_{26}\left[\mathrm{Cl^-}\right] + k_{30}[\mathrm{Cl_2^{\circ -}}])\end{aligned} \tag{24}$$

Considering that the oxidant is in a high level (i.e., $k_5[H_2O_2]\delta_{R_7} + k_5[H_2O_2]\delta_{R_8} \gg \sum k_i[X_i]$, where $\sum k_i[X_i] = k_6[HO_2^-] + k_8[HO_2^\circ]k_9[O_2^{\circ -}] + k_{14}[C]d + k_{17}[DOC] + k_{18}[CO_3^{2-}] + k_{19}[HCO_3^-] + k_{23}[HSO_4^-] + k_{26}[Cl^-] + k_{30}[Cl_2^{\circ -}])$ and $2\phi_{H_2O_2} I_{a,H_2O_2}\delta_{R_3} + 2\phi_{HO_2^-} I_{a,HO_2^-}\delta_{R_4} \gg \sum(k_{11}[H_2O_2][HO_2^\circ] + k_{12}[H_2O_2][O_2^{\circ -}]$, Eq. (24) can be simplified to Eq. (25) (prediction model C). k_i and $[X_i]$ are the reaction rate constants between HO° and species *i*, and the concentration of species *i*, respectively.

$$[\mathrm{HO}^\circ] = \frac{2\phi_{\mathrm{H_2O_2}} I_{a,\,\mathrm{H_2O_2}} \delta_{R_3} + 2\phi_{\mathrm{HO_2^-}} I_{a,\,\mathrm{HO_2^-}} \delta_{R_4}}{k_5[\mathrm{H_2O_2}]\delta_{R_7} + k_5[\mathrm{H_2O_2}]\delta_{R_8}} \tag{25}$$

The initial values of DOC and inorganic anionic species (CO_3^{2-}, HCO_3^-, SO_4^{2-}, Cl^-, etc.) are set according to the conditions of the water to be treated.

2.3. Numerical solution of the proposed kinetic models

The ODE system compiled in **Table 1** was solved applying MATLAB software and ODE15S function. For simultaneously solving the ODE set of the proposed kinetic models, it was necessary to define several photochemical parameters such as $\phi_{H_2O_2}$, $\phi_{pollutant}$, ϕ_{DOC}, $\varepsilon_{H_2O_2}$, $\varepsilon_{HO_2^-}$, $\varepsilon_{pollutant}$, ε_{DOC}, I_0 and l. Additionally, the initial concentrations of all the species involved in the system and the rate constants of the chemical reactions between those species were required (**Table 1**). During setting up the model, differential rate equations describing the time dependence of the concentration of the variety of the considered species were defined and plotted.

3. Results and discussion

In order to validate the proposed kinetic models, experimental data for PHE degradation by the UV/H_2O_2 process were used from Alnaizy and Akgerman [19] study. These authors conducted a set of experiments in a completely mixed batch cylindrical photoreactor made on Pyrex glass. The used photochemical parameters and the kinetic reaction rate constants of PHE with HO°, $O_2^{\circ-}$, and $CO_3^{\circ-}$ are presented in **Table 2**.

Parameters	Notation	Numerical values	References
Quantum yield	$\phi_{phenol} = \phi_C$	0.07 mol Ein^{-1}	[23]
Molar extinction coefficient	$\varepsilon_{phenol} = \varepsilon_C$	51 600 M^{-1} m^{-1}	[19]
Path length	l	63.5 mm	
Incident UV-light intensity (radiation of 254 nm > 90% and power = 15 W)	I_0	1.516×10^{-6} Ein L^{-1} s^{-1}	
Kinetic rate constant phenol-HO°	$k_{phenol,HO^\circ} = k_{14}$	6.6×10^9 M^{-1} s^{-1}	[40]
Kinetic rate constant phenol-$O_2^{\circ-}$	$k_{phenol,O_2^{\circ-}} = k_{16}$	5.8×10^3 M^{-1} s^{-1}	[41]
Kinetic rate constant phenol-$CO_3^{\circ-}$	$k_{phenol,CO_3^{\circ-}} = k_{35}$	2.2×10^7 $M^{-1}s^{-1}$	[42]

Table 2. Values of the parameters used in the kinetic model validation for phenol degradation.

3.1. Assumptions taken into consideration

As stated previously, the developed kinetic models A, B, and C employed the non-pseudo-steady, the pseudo-steady, and the simplified pseudo-steady state assumption, respectively, to estimate HO° concentration. In the proposed models, the impact of UV radiation individually

http://dx.doi.org/10.5772/65096

and/or the combined action of H_2O_2 and UV light (including the effect of HO°, HO_2°, O_2°$^-$, and CO_3°$^-$) on PHE degradation was studied.

A PHE concentration of 2.23×10^{-3} M and a H_2O_2/PHE ratio of 495 were selected for validating the model. The used PHE solution was prepared by adding the appropriate amount of pollutant solution to deionized water [19]. Therefore, the effect of inorganic anions, excluding HCO_3^- and CO_3^{2-} was not taken into account. In this sense, in the PHE degradation rate expression (ODE_1) the contribution of inorganic anion radicals, such as SO_4°$^-$, H_2ClO°, HClO°, Cl°, and Cl_2°$^-$, was not studied. It was assumed that the other terms included in ODE_1 contributed to pollutant degradation.

As the treated water was deionized, the presence of OM different from the parent compound in the initial solution was neglected ($[DOC]_0 = 0$ M). Hence, the DOC in the solution came from PHE photolysis and free radical (HO°, HO_2°, O_2°$^-$, and CO_3°$^-$) oxidation.

On the other hand, several authors agree that OM reduction by direct photolysis in a UV/H_2O_2 oxidation process can be neglected [7–9]. That is the reason why this was not included in the proposed kinetic model. However, it is highlighted that the OM is able to absorb UV-light, preventing UV-penetration into the bulk and avoiding H_2O_2/HO_2^- and pollutant direct photolysis. Therefore, the detrimental effect of UV-shielding in PHE degradation was taken into consideration. For including this effect in the kinetic model, OM molar extinction coefficient, referred as DOC molar extinction coefficient (ε_{DOC}), must be previously known. Although this parameter has already been measured [7, 8], its value is not a universal one, since DOM is a complex group of aromatic and aliphatic hydrocarbon structures with attached functional groups [20, 21]. As Alnaizy and Akgerman [19] did not measure this variable, a mean value from Peuravuori and Pihlaja [22] study was presumed. This value corresponded to $\varepsilon_{DOC(280\,nm)} = 35\,967\ M^{-1}\ m^{-1}$, which was in the same order of magnitude than ε_{PHE}. This number could be acceptable due to the formed aromatic intermediates during PHE conversion [19] conserve structural similarities with the parent compound, like the aromatic ring, responsible for the molecule excitation.

Additionally, it is widely known that the quantum yield of a compound is dependent on the excitation wavelength and the pH of the solution. For 254 nm, PHE quantum yield in an aqueous solution was found to be in the range of 0.02–0.12 mol Ein^{-1} at pH 1.6–3.2 [23]. Therefore, an average value (0.07 mol Ein^{-1}) was taken as PHE quantum yield.

Moreover, it is widely recognized that the solution pH decreases as the process proceeds. This variation in the pH can cause difficulties in modeling studies, since the presence of radical species such as HO_2°, and O_2°$^-$, among other chemical species involved in the oxidation system, is significantly dependent on the pH of the medium. Therefore, to give a more realistic view of what happens inside the reaction medium, H_2O_2 and HO_2^- photolysis reactions (Eqs. (1) and (2), correspondingly), as well as reactions expressed in Eqs. (26) and (27) were discriminated in the model according to the solution pH time evolution, as it is simplified in **Figure 3**. For selecting the suitable reactions with regard to the pH changes over time, previous information about the evolution of the pH during the performance of the process is required. However, in some occasions this is not provided. In this case, the initial pH of the solution was 6.8 [19]. At

this pH, one of the predominant species into the bulk was H_2O_2, since the pKa of the H_2O_2/HO_2^- equilibrium is 11.6. Therefore, the photolysis of HO_2^- was neglected in the model performance (i.e., δ_{R_3} and δ_{R_4}). Additionally, the initial concentrations of HO° and other considered species were assumed to be zero, with the exception of the pollutant and H_2O_2. On the other hand, it was found that the pH of the medium rapidly dropped from 6.8 to 4.7–4.2 (4.5 as a mean value) within the first 30 min of radiation [19]. Therefore, and according to **Figure 3**, Eq. (26) was considered during the first 30 min of the reaction while Eq. (27), after that time (i.e., $\delta_{R_7} = 1$, $\delta_{R_8} = 0$ and $\delta_{R_7} = 0$, $\delta_{R_8} = 1$, before and after the first 30 min of the process, respectively).

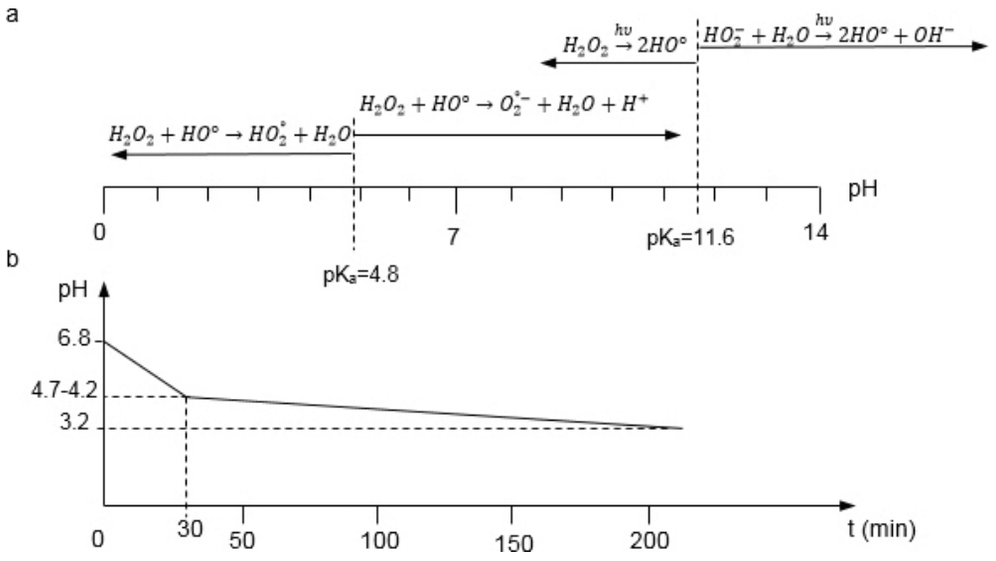

Figure 3. (a) Reaction discrimination diagram as a function of the solution pH and (b) pH evolution of the medium during the UV/H_2O_2 process in a completely mixed batch photoreactor. Operating conditions: H_2O_2/PHE = 495; $[C]_0$ = 2.23×10^{-3} M; t = 220 min.

$$O_2^{°-} + H^+ \rightarrow HO_2^° \tag{26}$$

$$H_2O_2 + HO^° \rightarrow O_2^{°-} + H_2O + H^+ \tag{27}$$

3.2. Kinetic model validation

Initially, the associated ODE sets with model A, B, and C were solved. Parameters $f = g = 0$ and $d = h = 1$ were considered in order to solely investigate the influence of the direct photolysis, HO°, and $CO_3^{°-}$ on PHE degradation.

http://dx.doi.org/10.5772/65096

Figure 4 compares the simulation results of the proposed kinetic models A, B, and C with the experimental data for 2.23 × 10^{-3} M PHE with a H_2O_2/PHE ratio of 495 and a reaction time of 220 min. The measured and simulated results for PHE direct photolysis alone are also presented. It is observed that more than 90% of the initial PHE concentration was removed after 220 min due to both direct photolysis and indirect degradation (primarily due to HO° attack). The effect of $CO_3^{\circ-}$ could be seen as marginal because of the reduced number of those radicals, in the range of 10^{-15} M, and the low reaction rate constant with PHE compared to HO°. In addition, it is shown that PHE was not completely removed by direct UV photolysis under the tested photochemical conditions (**Table 2**), since approximately 50% of the total PHE degradation was attributed to UV photolysis, as it was experimentally determined by Alnaizy and Akgerman [19]. On the other hand, the figure demonstrates that the prediction kinetic model C was in good agreement with the available experimental data with a relative high correlation factor (R^2=99.34%). For prediction models A and B, R^2 were 97.41 and 97.37%, respectively. As a result of the subtle differences between kinetic models A and B, the depicted line describing model A overlaps model B line. An acceptable agreement between model predictions considering only the UV radiation and experimental data was also verified (R^2 = 98.25%).

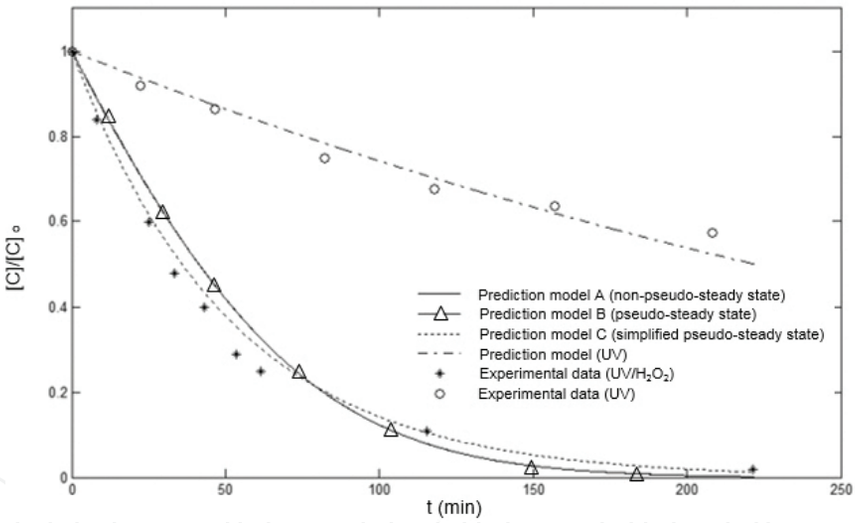

Figure 4. Comparison of the kinetic model predictions (lines) versus experimental data (o) and (*). Operating conditions: H_2O_2/PHE = 495; $[C]_0$ = 2.23 × 10^{-3} M; t = 220 min.

Furthermore, **Figure 4** clearly presents that the removal rate of the target pollutant was not significantly dependent on the hypothesis assumed to estimate the HO° level (non-pseudo-steady, pseudo-steady and simplified pseudo-steady state assumptions). This could be explained from the relatively low concentration of those reactive species in the solution (with a magnitude order of 10^{-14} M) when compared to the level of other species involved in the system, such as HO_2° and $O_2^{\circ-}$, whose concentrations were in the range of 10^{-7} M. The number of HO° remaining in the solution is in concordance with the low final HO° levels found in the literature [24, 25] and even higher than those reported by Ray and Tarr [26].

In **Figure 5**, the evolution of the HO°, HO_2°, O_2°$^-$, DOC and $H_2CO_3^*$ normalized estimated concentrations using the prediction model A is depicted. It is observed that HO_2° number increased as the oxidation system proceeded, while O_2°$^-$ level decreased. Typically, the effect of HO_2° and O_2°$^-$ radicals are neglected in the UV/H_2O_2 system [6–8, 15, 17, 27, 28] since they are found to be less reactive than HO°, as stated previously. However, when they are produced in a high level, they could also participate in the contaminant oxidation. That is the current case of HO_2°, as [HO_2°] >>>> [HO°]. Therefore, the contribution of HO_2° to PHE degradation should be studied. On the other hand, in this work the action of O_2°- in PHE conversion can be omitted since O_2°- level decreased with the reaction time, as expected, because of the drop in the pH solution.

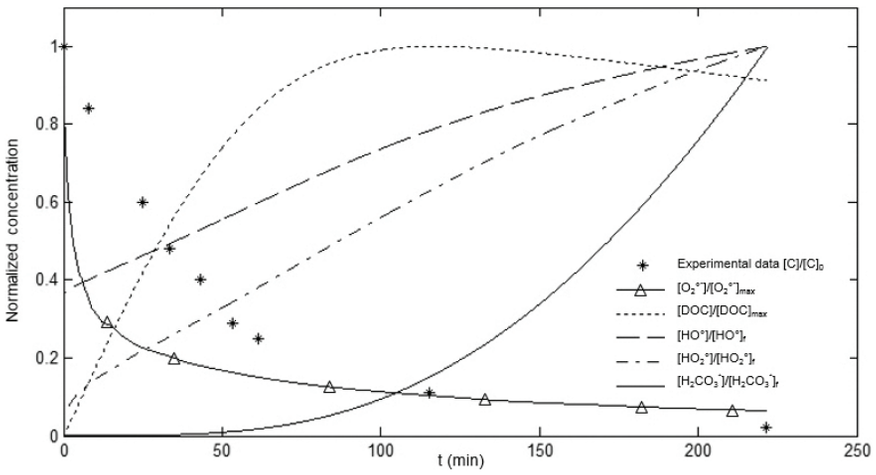

Figure 5. Concentration-time profiles of HO° (---), HO_2° (-.-.-), O_2°− (-Δ-), DOC (···) and $H_2CO_3^*$ (—) using the prediction kinetic model A. (*) represents PHE experimental evolution. Operating conditions: H_2O_2/PHE = 495; $[C]_0$ = 2.23 × 10^{-3} M; *t* = 220 min.

Furthermore, generally, there is a drop in the pH of the medium as the system progresses. This is probably due to acidic compound formation, such as carboxylic acids and $H_2CO_3^*$ resulting from pollutant degradation and mineralization. In this study the decrease of the pH in the solution was predicted via DOC conversion and the sole generation of $H_2CO_3^*$ by model A. As presented in **Figure 5**, DOC generation was progressively increasing as PHE was being degraded up to a certain point (117 min, corresponding to $[DOC]_{max}$ = 2.061 × 10^{-3} M, and equivalent to ca. 93% of PHE degradation). From this point, DOC started to decrease until $[DOC]_f$ = 1.879 × 10^{-3} M. That breakpoint represented the moment at which PHE was almost completely transformed into by-products. In addition, at this point, PHE mineralization began to be more evident, since $H_2CO_3^*$ level rose approximately in a linear way, up to a final level of 6.493 × 10^{-14} M, with the subsequent pH decrease. Similarities between the pattern of this DOC profile and that of the formed intermediate curves reported in Alnaizy and Akgerman [19] research are highlighted.

On the other hand, it is worth noting that HO° level evolution with the reaction time was different when comparing the kinetic prediction model A or B with C. Obviating HO_2° contribution to PHE degradation, **Figure 6** shows that the highest final HO° level was achieved

http://dx.doi.org/10.5772/65096

in the prediction model A, with a maximum HO° concentration equal to 9.435×10^{-14} M. This value was similar to HO° final level in the prediction model B (9.400×10^{-14} M) and different to that of the prediction model C, where HO° final concentration was 4.486×10^{-14} M (ca. 48% lower than the obtained in the kinetic model A or B).

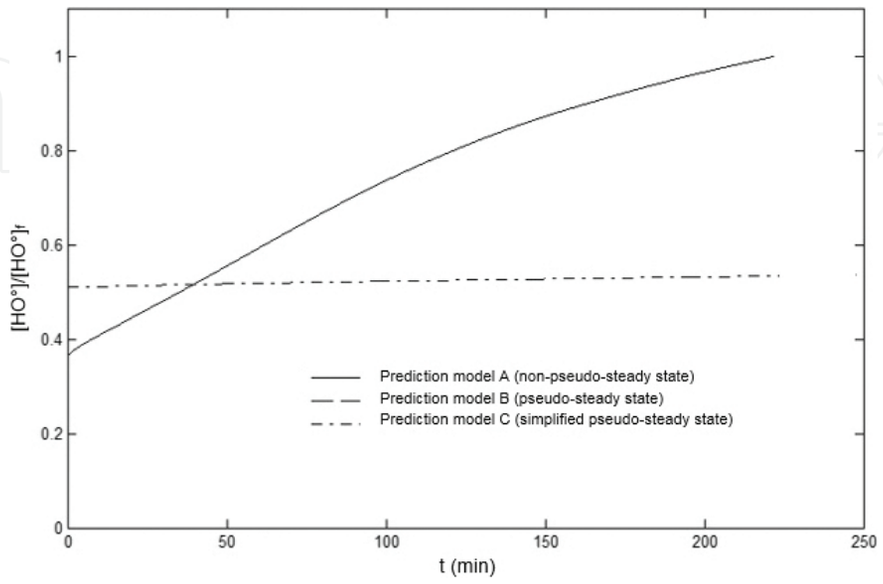

Figure 6. Estimated HO° concentration using the prediction models A (——), B (----), and C (-.-.-). Operating conditions: H_2O_2/PHE = 495; $[C]_0 = 2.23 \times 10^{-3}$ M; t = 220 min.

Approximately, in the first 40 min of the process a larger number of HO° in the aqueous medium with the developed kinetic model C was evidenced. Apparently, this amount of HO° was sufficient to degrade about 60% of PHE initial level under the studied experimental conditions. In contrast, models A and B, whose lines are overlapped, produced a lower number of HO° and the theoretical conversion of PHE remained above the experimental data. One possible reason for this discrepancy can be ascribed to DOM and dissolved oxygen positive effects in producing reactive oxygen species (ROS), as HO° [26], which were not considered. After 40 min of reaction, the HO° level was higher in the kinetic models A and B than in model C. This larger amount of HO° might lead to a faster conversion of the pollutant in comparison with the predicted model C, since the hypothetical depletion curve of PHE was below the measured data. Nevertheless, this rapid pollutant degradation did not occur actually. Therefore, there was an amount of HO° produced in excess that was not reacting with the contaminant. This surplus of HO° could be involved in free radical scavenging reactions. As model A and B consider the detrimental effect of HO° consuming reactions, it is suggested that their kinetic rate constants are higher than those ones used in this paper for these reactions to have a larger weight in the system. Additionally, the contradictory outcome between the actual situation and the theoretical one in the first and second stage of the process can also be attributed to the fact that just a fraction of the concentration of the species involved in the whole kinetic equations of the predicted models was actually reacting. Consequently, the real level of the species implicated in each kinetic reaction

should be considered. However, it is rather difficult to determine which amount of the chemical species is exactly involving in each reaction for each time step, especially due to the high reactivity of radicals as the oxidation system progresses. In this context, further studies are required to overcome this limitation.

From these findings, it is suggested that there was an effective level of the formed HO°. Below that level, there was a lack of HO° for an efficient pollutant conversion; and above it, an excessive number of HO° was generated. That HO° effective level could be of relevance for industrial applications in order to be maintained throughout the reaction time, allowing an efficient pollutant degradation.

3.3. Estimation of PHE-HO_2° reaction rate constant

In order to study the action of HO_2° for pollutant degradation in the UV/H_2O_2 system, PHE-HO_2° rate constant was calculated. For this purpose, the kinetic model A was used and it was estimated through a non-linear least-square objective function. The objective function for minimizing the error between the predicted and the measured data was defined as Eq. (28) [17].

$$\text{Minimize}: f = \sum \left([\mathrm{C}]_{\text{predicted}} - [\mathrm{C}]_{\text{measured}} \right)^2 \tag{28}$$

where $[\mathrm{C}]_{\text{measured}}$ and $[\mathrm{C}]_{\text{predicted}}$ correspond to the evolution of experimental and calculated pollutant concentration, respectively. This expression is a function of PHE-HO_2° rate constant. The optimum value for PHE-HO_2° second-order rate constant was found to be 1.6×10^3 M^{-1} s^{-1}, which is consistent with the range of the reported values by Kozmér et al. ($(2.7 \pm 1.2) \times 10^3$ M^{-1} s^{-1}) [29]. The results of running the new prediction kinetic model A (with and without the contribution of HO_2° to pollutant conversion) and the experimental data are presented in **Figure 7**. The figure shows that the prediction model A with the estimation

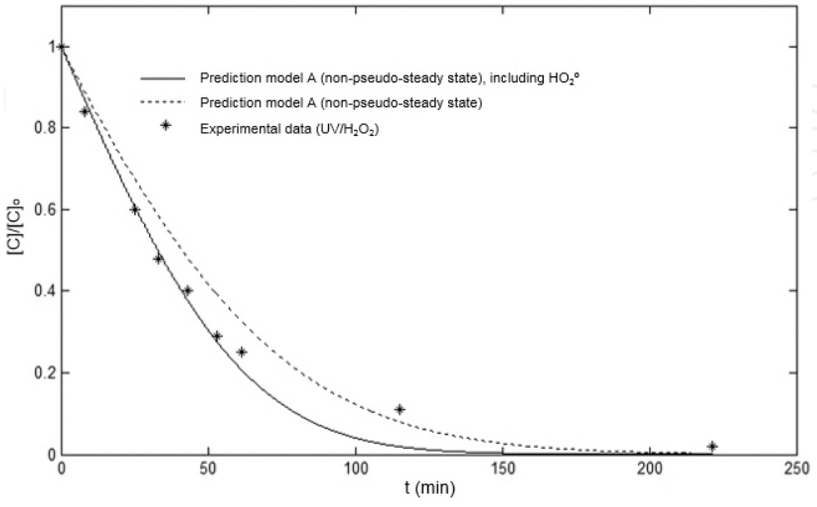

Figure 7. Comparison of experimental (symbols) vs predicted data (lines) using the kinetic model A with (—) and without (···) the action of HO_2°. Operating conditions: H_2O_2/PHE = 495; $[C]_0 = 2.23 \times 10^{-3}$ M; t = 220 min.

http://dx.doi.org/10.5772/65096

of PHE-HO_2° rate constant was in a stronger agreement with the experimental data (R^2 = 99.0%) than the previous predicted kinetic model A studied in section 3.2 (R^2 = 97.41%). The same conclusion can be drawn for kinetic model B and C, with a R^2 of 98.78 and 99.57% using the calculated PHE-HO_2° rate constant, in comparison with 97.37 and 99.34%, respectively. Therefore, in order to achieve a better fit between experimental and predicted data, HO_2° action in pollutant degradation should be considered. Nonetheless, HO_2° contribution to PHE degradation is non-significant in comparison with the role developed by HO° attack.

4. Conclusions

A kinetic model for studying pollutant degradation by the UV/H_2O_2 system was developed, including the background matrix effect in scavenging free radicals and shielding UV-light and the reaction intermediate action, as well as the change of the pH as the UV/H_2O_2 process proceeds. Three different ways for calculating HO° level time evolution were assumed (non-pseudo-steady, pseudo-steady and simplified pseudo-steady state; denoted as kinetic models A, B, and C, respectively). It was found that the assumption of pseudo-steady (simplified or not) or transient state for determining the HO° level evolution with time was not significant in PHE degradation rate due to the relatively low HO° level present into the bulk (~10^{-14} M). On the other hand, taking into account the high levels of HO_2° formed in the reaction solution compared to HO° concentration (~10^{-7} M >>>> ~10^{-14} M), HO_2° action in transforming PHE was considered. For this purpose, PHE-HO_2° reaction rate constant was calculated and estimated to be 1.6 × 10^3 M^{-1} s^{-1}, resulting in the range of data reported from literature. It was observed that, although including HO_2° action allowed slightly improving the kinetic model degree of fit, HO° developed the major role in PHE conversion, due to their high oxidation potential.

Additionally, it was found that there was an effective level of the HO° formed in solution. Below that level, there was a lack of HO° for an efficient pollutant conversion; and above it, an excessive number of HO° was generated. That HO° effective level calculated from kinetic model C could be of relevance for industrial applications in order to be maintained throughout the reaction time, allowing an efficient pollutant degradation.

In this study, there was an attempt to contemplate a wide range of the chemical reactions involved in the UV/H_2O_2 process and although high correlation factors were obtained, it is suggested to include the positive effect of the OM and the dissolved oxygen in generating ROS, as well as the effect of other anions naturally present in water bodies, as phosphate and nitrate, for the model to be a more accurate approximation of reality.

Acknowledgements

This work was financially supported by the Colombian Administrative Department of Science, Technology and Innovation (COLCIENCIAS).

Author details

Ainhoa Rubio-Clemente[1,2*], E. Chica[3] and Gustavo A. Peñuela[1]

*Address all correspondence to: ainhoarubioclem@gmail.com

1 Grupo GDCON, Facultad de Ingeniería, Sede de Investigaciones Universitarias (SIU), Universidad de Antioquia UdeA, Colombia

2 Departamento de Ciencia y Tecnología de los Alimentos, Facultad de Ciencias de la Salud, Universidad Católica San Antonio de Murcia UCAM, Spain

3 Departamento de Ingeniería Mecánica, Facultad de Ingeniería, Universidad de Antioquia UdeA, Colombia

References

[1] Rubio-Clemente, A., Torres-Palma, R.A., & Peñuela, G.A. Removal of polycyclic aromatic hydrocarbons in aqueous environment by chemical treatments: A review. Sci. Total Environ. 2014;408:201–225.

[2] Rubio-Clemente, A., Chica, E., & Peñuela, G.A. Application of Fenton process for treating petrochemical wastewater. Ingeniería y Competitividad. 2014;16(2): 211–223.

[3] Rubio-Clemente, A., Chica, E., & Peñuela, G.A. Petrochemical wastewater treatment by photo-Fenton process. Water, Air, Soil Pollut. 2015;226(3):61–78.

[4] Dopar, M., Kušić, H, & Koprivanac, N. Treatment of simulated industrial wastewater by photo-Fenton process: Part I: The optimization of process parameters using design of experiments (DOE). Chem. Eng. J. 2011;173:267–279.

[5] Litter, M., & Quici, N. Photochemical advanced oxidation processes for water and wastewater treatment. Recent Pat. Eng. 2010;4:217–241.

[6] Wols, B.A., & Hofman-Caris, C.H.M. Review of photochemical reaction constants of organic micropollutants required for UV advanced oxidation processes in water. Water Res. 2012;46:2815–2827.

[7] Song, W., Ravindran, V., & Pirbazari, M. Process optimization using a kinetic model for the ultraviolet radiation-hydrogen peroxide decomposition of natural and synthetic organic compounds in groundwater. Chem. Eng. Sci. 2008;63:3249–3270.

[8] Audenaert, W.T.M., Vermeersch, Y., Van Hulle, S.W.H., Dejans, P., Dumoulin, A., & Nopens, I. Application of a mechanistic UV/hydrogen peroxide model at full-scale:

Sensitivity analysis, calibration and performance evaluation. Chem. Eng. J. 2011;171:113–126.

[9] Crittenden, J.C., Hu, S., Hand, D.W., & Green, S.A. A kinetic model for H2O2/UV process in a completely mixed batch reactor. Water Res. 1999;33(10):2315–2328.

[10] Hong, A., Zappi, M.E., & Hill, D. Modeling kinetics of illuminated and dark advanced oxidation processes. J. Environ. Eng. 1996;122(1):58–62.

[11] Huang, C.R., & Shu, H.Y. The reaction kinetics, decomposition pathways and intermediate formation of phenol in ozonation, UV/O_3 and UV/H_2O_2 processes. J. Hazard. Mater. 1995;41:47–64.

[12] Liao, C.H., & Gurol, M.D. Chemical oxidation by photolytic decomposition of hydrogen peroxide. Environ. Sci. Technol. 1995;29(12):3007–3014.

[13] Primo, O., Rivero, M.J., Ortiz, I., & Irabien, A. Mathematical modelling of phenol photooxidation: Kinetics of the process toxicity. Chem. Eng. J. 2007;134(1–3):23–28.

[14] Rosenfeldt, E.J., & Linden, K.G. The ROH,UV concept to characterize and the model UV/H2O2 process in natural waters. Environ. Sci. Technol. 2007;41(7):2548–2553.

[15] Yao, H., Sun, P., Minakata, D., Crittenden, J.C., & Huang, C.H. Kinetics and modeling of degradation of ionophore antiobiotics by UV and UV/H2O2. Environ. Sci. Technol. 2013;47(9):4581–4589.

[16] Zeng, Y., Hong, P.K.A., & Wavrek, D.A. Integrated chemical-biological treatment of benzo(a)pyrene. Environ. Sci. Technol. 2000;34(5):854–862.

[17] Edalatmanesh, M., Dhib, R., & Mehrvar, M. Kinetic modeling of aqueous phenol degradation by UV/H_2O_2 process. Int. J. Chem. Kinet. 2007;40(1):34–43.

[18] De Laat, J., Le, G.T., & Legube, B. A comparative study of the effects of chloride, sulfate and nitrate ions on the rates of decomposition of H_2O_2 and organic compounds by Fe(II)/H_2O_2 and Fe(III)/H_2O_2. Chemosphere. 2004;55(5):715–723.

[19] Alnaizy, R., & Akgerman, A. Advanced oxidation of phenolic compounds. Adv. Environ. Res. 2000;4(3):233–244.

[20] Leenheer, J.A., & Croué, J.P. Characterizing aquatic organic matter: Understanding the unknown structures is key to better treatment of drinking water. Environ. Sci. Technol. 2003;37(1):18A–26A.

[21] Wang, Z., Wu, Z., & Tang, S. Characterization of dissolved organic matter in a submerged membrane bioreactor by using three-dimensional excitation and emission matrix fluorescence spectroscopy. Water Res. 2009;43(6):1533–1540.

[22] Peuravuori, J., & Pihlaja, K. Molecular size distribution and spectroscopic properties of aquatic humic substances. Anal. Chim. Acta. 1997;337(2):133–149.

[23] Alapi, T., & Dombi, A. Comparative study of the UV and UV/VUV-induced photolysis of phenol in aqueous solution. J. Photochem. Photobiol. A. 2007;188((2–3)):409–418.

[24] Gallard, H., & De Laat, J. Kinetic modelling of Fe(III)/H_2O_2 oxidation reactions in dilute aqueous solution using atrazine as a model organic compound. Water Res. 2000;34(12): 3107–3116.

[25] Rosenfeldt, E.J., Linden, K.G., Canonica, S., & von Gunten, U. Comparison of the efficiency of °OH radical formation during ozonation and the advanced oxidation processes O_3/H_2O_2 and UV/H_2O_2. Water Res. 2006;40(20):3695–3704.

[26] Ray, P.Z., & Tarr, M.A. Petroleum films exposed to sunlight produce hydroxyl radical. Chemosphere. 2014;103:220–227.

[27] Kralik, P., Kušić, H., Koprivanac, N., & Božić, A.L. Degradation of chlorinated hydrocarbons by UV/H_2O_2: The application of experimental design and kinetic modeling approach. Chem. Eng. J. 2010;158(2):154–166.

[28] Kušić, H., Koprivanac, N., Božić, A.L., Papić, S, Peternel, I., & Vujević, D. Reactive dye degradation by AOPs: Development of a kinetic model for UV/H_2O_2 process. Chem. Biochem. Eng. Q. 2006;20(3):293–300.

[29] Kozmér, Z., Arany, E., Alapi, T., Takács, E., Wojnárovits, L., & Dombi, A. Determination of the rate constant of hydroperoxyl radical reaction with phenol. Radiat. Phys. Chem. 2014;102:135–138.

[30] Bielski, B.H.J., Cabelli, D.E., Arudi, L.R., & Ross, A.B. Reactivity of HO_2/O_2^- radicals in aqueous solution. J. Phys. Chem. Ref. Data. 1985;14(4):1041–1100.

[31] Buxton, G.V., Greenstock, C.L., Helman, W.P., & Ross, A.B. Critical review of data constants for reactions of hydrated electrons, hydrogen atoms and hydroxyl radicals in aqueous solutions. J. Phys. Chem. Ref. Data. 1988;17(2): 513–886.

[32] Christensen, H.S., Sehested, K., & Corftizan, H. Reaction of hydroxyl radicals with hydrogen peroxide at ambient temperatures. J. Phys. Chem. 1982;86:15–88.

[33] Schested, K., Rasmussen, O.L., & Fricke, H. Rate constants of OH with HO_2, O_2^- and H_2O_2+ from hydrogen peroxide formation in pulse-irradiated oxygenated water. J. Phys. Chem. 1968;72:626–631.

[34] Weinstein, J., Benon, H.J., & Bielski, H.J. Kinetics of the interaction of HO_2 and O_2-radicals with hydrogen peroxide. The Haber-Weiss reaction. J. Amer. Chem. Soc. 1979;101:58–62.

http://dx.doi.org/10.5772/65096

[35] Wols, B.A., Harmsen, D.J.H., Beerendonk, E.F., & Hofman-Caris, C.H.M. Predicting pharmaceutical degradation by UV (LP)/H_2O_2 processes: A kinetic model. Chem. Eng. J. 2014;255:334–343.

[36] Draganic, Z.D., Negron-Mendoza, A., Sehested, K., Vujosevic, S.I., Navarro-Gonzales, R., Albarran-Sanchez, M.G. Radiolysis of aqueous solutions of ammonium bicarbonate over a large dose range. Radiat. Phys. Chem. 1991;38(3):317–321.

[37] Neta, P., Huie, R.E., & Ross, A.B. Rate constants for reactions of inorganic radicals in aqueous solution. J. Phys. Chem. Ref. Data. 1988;17(3):1027–1284.

[38] Fang, G.D., Dionysiou, D.D., Wang, Y., Al-Abed, S.R., & Zhou, D.M. Sulfate radical-based degradation of polychlorinated biphenyls: Effects of chloride ion and reaction kinetics. J. Hazard. Mater. 2012;227–228:394–401.

[39] Mazellier, P., Leroy, É., De Laat, J., & Legube, B. Transformation of carbendazim induced by the H_2O_2/UV system in the presence of hydrogenocarbonate ions: Involvement of the carbonate radical. New J. Chem. 2002;26(12):1784–1790.

[40] Dorfman, L.M., & Adams, G.E. Reactivity of the hydroxyl radical in aqueous solutions. Standard Reference Data System. National Bureau of Standards and Technology. 1973;46.

[41] Yasuhisa, T., Hideki, H., & Muneyoshi, Y. Superoxide radical scavenging activity of phenolic compounds. Int. J. Biochem. 1993;25(4):491–494.

[42] Chen, S.N., & Hoffman M.Z. Rate constants for the reaction of the carbonate radical with compounds of biochemical interest in neutral aqueous solution. Radiat. Res. 1973;56(1):40–47.

IntechOpen